Supplemental Inventory

- Supplemental Figure S1, related to Figures 1 to 3:
It concerns additional phenotypes of the mutants described in Figures 1 to 3.

- Supplemental Figure S2, related to Figures 1 to 3:
Recombination defects of the mutants described in Figures 1 to 3.

- Supplemental Figure S3, related to Figure 4:
Mer3 localization in *msh4Δ* mutant and leptotene phenotype of *mer3Δ msh4Δ* double mutant.

- Supplemental Experimental Procedures

- Supplemental Reference

Supplemental Extended Experimental Procedures

Cloning and Sequencing

Primers design was based on *Neurospora crassa* sequences (http://www.broad.mit.edu/) and *Sordaria macrospora MER3, MLH1 and MSH4* (GenBank accession numbers FJ528581, FJ528583, FJ528582.1) were identified by PCR from an indexed genomic library. Double-strand sequences were obtained using specific primers (Sigma-Genosys or Primm).

Strains, Plasmids and Transformation of Sordaria

The homothallic *S. macrospora* WT strain is "St Ismier" strain FGSC 4818. Transformations with recombinant DNA to obtain the deletion mutants were performed in a *ku70*□ mutant background, which increases the homologous integration events. In all mutants (*mer3*□, *mlh1*□, and *msh4*□) a hygromycin resistance cassette replaces the coding region exactly from ATG to the stop codon. The exogenous DNA used to transform Sordaria includes about 1kb regions of homology at both 3' and 5' of the gene of interest. Gene deletions were confirmed by Southern blotting and PCR. All the deleted alleles were subsequently introduced in a *KU70* WT background by genetic crosses.

Sordaria Mer3 helicase motif I (aa 294-298, GSGKT) is 100% identical to the *S. cerevisiae* domain. The *mer3*KA mutation (K297A) was created by PCR-based mutagenesis (oligos used were: MerKAFor: CCAACAGGAAGCGGC**gc**AACAGCCATCCTG; and MerKArev: CAGGATGGCTGTT**gc**GCCGCTTCCTGTTGG). Sordaria strains carrying the mutant allele were selected by co-transformation with a plasmid encoding the nourseothricine resistance (details available upon request).

C-terminally GFP-tagged versions of the genes, under control of their promoters, were introduced at ectopic locations into a WT strain and further crossed to the null strains of interest. Msh4-GFP and Mer3-GFP proteins are fully functional: (i) they complement all meiotic defects of their cognate null mutants; (ii) like WT, the complemented strains produce exclusively 8-spored asci with

95% viable ascospores for Mer3-GFP and 99% for Msh4-GFP and WT (n = 22 asci for each strain). Moreover, localization and numbers of both Msh4 and Mer3 foci are similar in WT and in null mutant backgrounds. No GFP immunostaining is detectable in strains lacking the GFP-fusion proteins. Unfortunately we could not detect focus formation by C- or N-terminally GFP-tagged *MLH1* or by anti-Mlh1 antibodies, including a Sordaria-specific one.

Interfocus Distances

Using straight axis segments with 5-12 foci, we measured the distance from the center of the first focus to the center of the next focus and the total length from the first to the last focus (with ImageJ). Total segment length obtained by adding individual adjacent distances was not different from that measured from the first to the last focus (e.g. a line with 5 foci average 2.5 ± 0.1 mm, t-Test: p=0.4 for Mer3-GFP, p=0.3 for Msh4-GFP foci). The □ parameter of the Gamma distribution fitted against interfocus-distances was computed using maximum likelihood fitting using the Wessa Gamma Distribution calculator: http://www.wessa.net/rwasp_fitdistrgamma .wasp/.

Inter-Homolog Matching Foci

To test whether foci "match" across homologs, we introduced the null hypothesis H_0 whereby foci positions on two chromosomes are not more correlated on homologs than on non-homologs. The experimental data list five consecutive focus positions for each of 61 pairs of coaligned homologs. To measure the correlation inside a pair, we scored the distances between foci of the same rank. The origin was set at the first focus and the scale normalized, bringing the five positions to 0, x_1, x_2, x_3, 1 (and 0, x'_1, x'_2, x'_3, 1 for the other homolog). Our score is then: $S = \sum_{i=1}^{3} (x_i - x'_i)^2$.

The "total" score □ is defined as the sum of these S over all homolog pairs. Under H_0, x'_i is independent of x_i. Let □* be the value of this total score for the 61 pairs of experimental homologous segments. We obtained a *p*-value for

H_0 by re-sampling: the different segments were shuffled 10^7 times and paired with random partners. For each such shuffle, we computed the corresponding □, and the *p*-value of H_0 was taken as the fraction of shuffles with □ < □*. We obtained a *p*-value of 0.0026, which excludes the hypothesis H_0.

Supplemental Information Figures and Legends

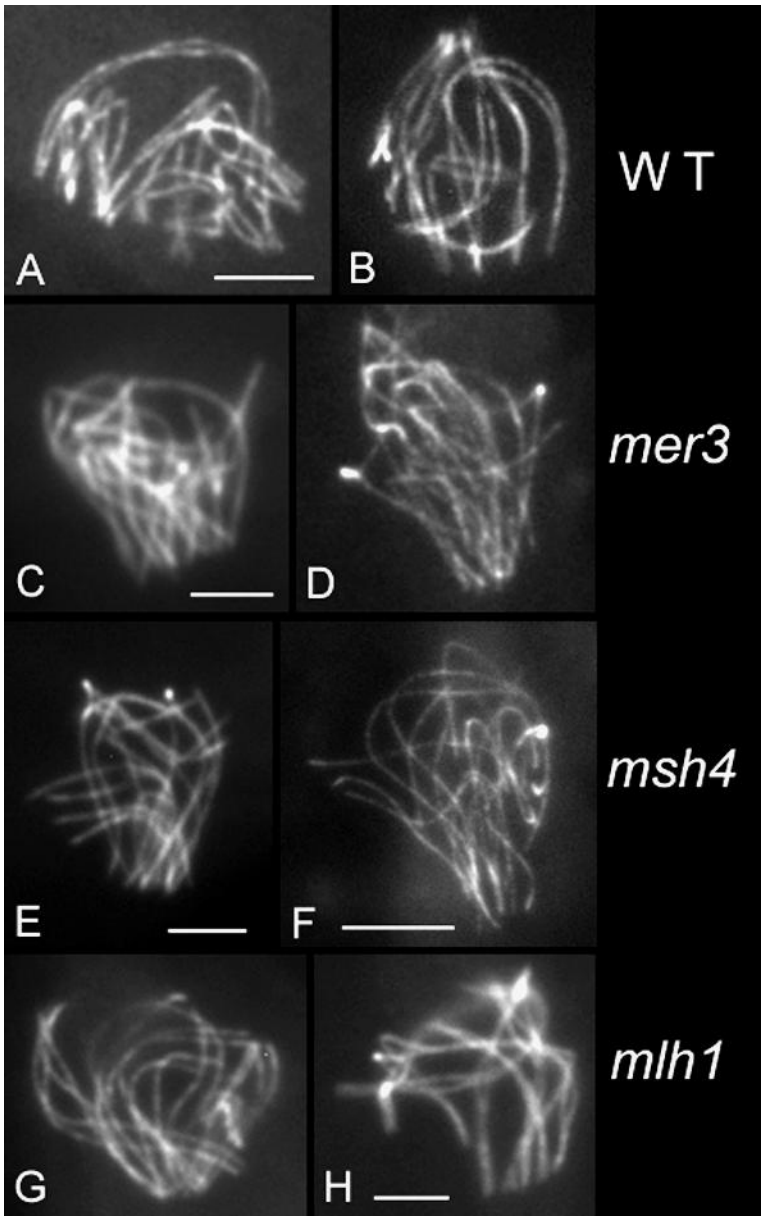

Figure S1. Bouquets in WT and Mutants - Related to Figures 1, 2 and 3

All three mutants form a bouquet at late leptotene (by ascus size) but exhibit delayed bouquet exit. In WT, bouquet stages never exceed 5-10% of all prophases (n = 900). In contrast, all three mutants show high frequencies of bouquets among total prophase nuclei (165 among 500 for *mer3*□; 158 of 520 for *msh4*□ and 162 of 505 for *mlh1*□; P<0.0001 in each case). Since bouquet formation starts normally, these increases imply delayed bouquet exit.

(A and B) Late leptotene and early zygotene bouquet configurations in WT. Note that almost all chromosome ends are first loosely (A) and later tightly (B) clustered in a limited area of the nuclear envelope.

(C and D) In *mer3*□, since pairing is delayed, chromosomes form a loose bouquet (C) before alignment and their ends are only partially clustered. Even at what should be early pachytene by ascus size, although tight bouquet formation (D), mostly only one chromosome end is in the cluster.

(E and F) In *msh4*□, homologs enter bouquet partially aligned (E) and form a tight bouquet (F) at the 600nm alignment stage.

(G and H) Early *mlh1*□ bouquet (G) shows completely aligned and (H) synchronously synapsing homologs like in WT (A and B). Bars, 2□m.

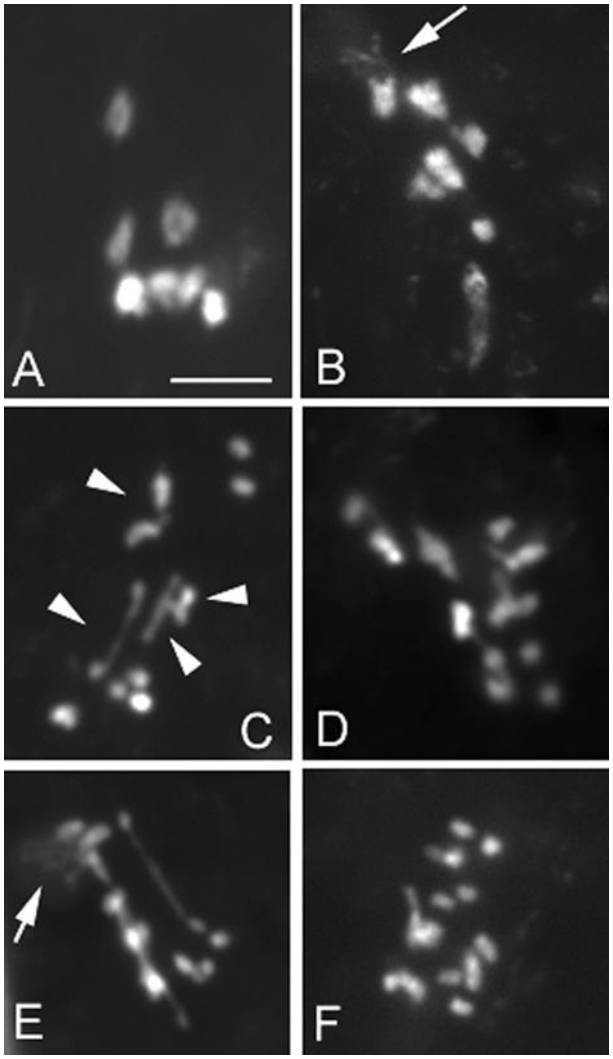

Figure S2. WT and Mutant Diplotenes - Related to Figures 1, 2 and 3

(A–F) Chromosomes are stained by DAPI.

(A) WT shows 7 chiasmate bivalents at late diplotene (mean chiasma number = 21 ± 3; n = 100).

(B) 41 among 43 *mlh1*□ diplotenes show seven bivalents like in WT but with reduced (~ 45%) chiasma numbers (arrow points to the nucleolar organizer region (NOR) of bivalent 2). This reduction is confirmed by genetic analysis: the second division segregation frequency of the spore color gene *PAM2*, which measures the frequency of a CO between this marker and the centromere of chromosome 4, is 60.8 % in WT (286 of the 470 ordered tetrads) and 24.6% (69 of 280 tetrads) in *mlh1*□. However, the frequency of non-Mendelian segregation (6:2 or 2:6 asci), as determined in an *mlh1*□ *PAM2* by *mlh1*□ *pam2* cross, is

similar to WT: 3 in 280 tetrads (1.1 %), compared to 6 among 470 tetrads (1.3 %), respectively. Thus, in *mlh1*□, while CO/chiasmata are reduced, NCOs appear to form normally.

(C) *msh4*□ and (D) *mer3*□ diplotenes. Both show a mixture of univalents and bivalents (arrowheads in C): note that these latter are mostly rod-shaped, indication of the presence of one chiasma, compared to the ring-shaped bivalents seen in WT (A). Among 50 diplotenes analyzed for each mutant, 26% exhibited 14 univalents and the remainder 74% exhibited a mixture of univalents and, respectively, 4-6 and 5-7 residual chiasmata per nucleus.

(E) *msh4*□ *mlh1*□ diplotenes show 3-6 chiasmata (n = 30): the two chromosomes 2 (arrow) have no chiasmata as indicated by the fact that the two NORs are separated.

(F) Example of a diplotene nucleus with 14 univalents in *msh4*□ *mer3*□. Bar, 2□m.

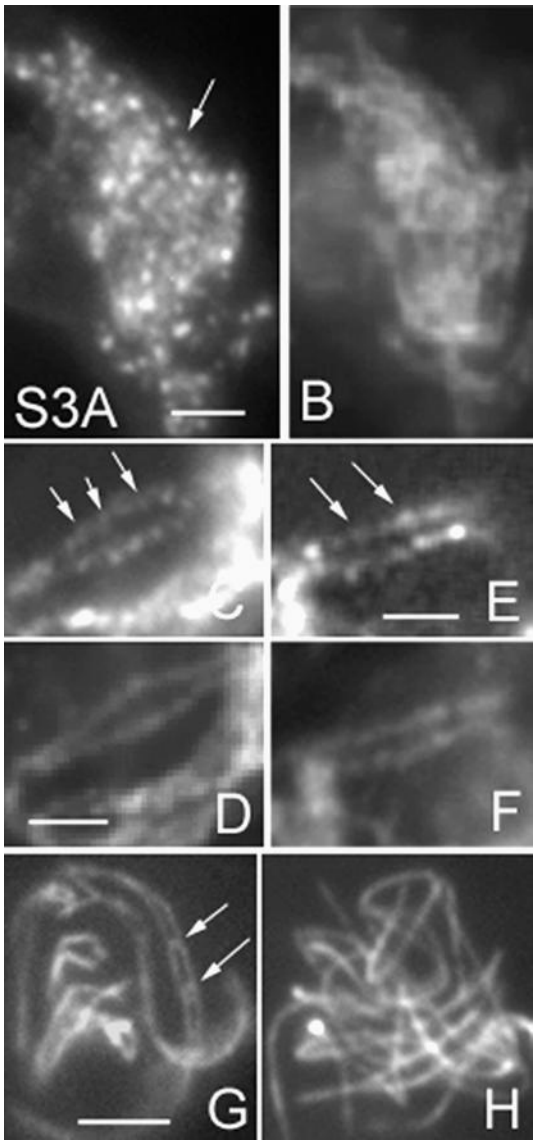

Figure S3. Mer3 localization in *msh4*□ and *mer3*□ *msh4*□ phenotype - Related to Figure 4

(A-G) Mer3-GFP foci in *msh4*□ show the same patterns as described for WT (text).

(A) Foci are seen on axes at early leptotene and are evenly spaced like in WT (arrow). (B) Corresponding DAPI.

(C - F) Foci are located on matching sites on aligned homologs (arrows in C and E). (D and F) Corresponding DAPI.

(G) Costaining with Spo76-GFP shows that, like in WT, Mer3 foci are delocalized from axes to the mid-axis zone in synapsing regions at zygotene (arrows).

(H) The *mer3*□ *msh4*□ double mutant shows both discoordinated alignment and interwoven chromosomes like *mer3*□. Bars, 2□m.